

A comparison of observed and predicted ground motions from the 2015 M_W 7.8 Gorkha, Nepal, earthquake

Susan E. Hough¹ · Stacey S. Martin² · Vineet Gahalaut³ · Anand Joshi⁴ · M. Landes⁵ · R. Bossu⁵

Received: 11 May 2016 / Accepted: 28 July 2016 / Published online: 16 August 2016
© Springer Science+Business Media Dordrecht (outside the USA) 2016

Abstract We use 21 strong motion recordings from Nepal and India for the 25 April 2015 moment magnitude (M_W) 7.8 Gorkha, Nepal, earthquake together with the extensive macroseismic intensity data set presented by Martin et al. (Seism Res Lett 87:957–962, 2015) to analyse the distribution of ground motions at near-field and regional distances. We show that the data are consistent with the instrumental peak ground acceleration (PGA) versus macroseismic intensity relationship developed by Worden et al. (Bull Seism Soc Am 102:204–221, 2012), and use this relationship to estimate peak ground acceleration from intensities (PGA_{EMS}). For nearest-fault distances ($R_{RUP} < 200$ km), PGA_{EMS} is

Electronic supplementary material The online version of this article (doi:10.1007/s11069-016-2505-8) contains supplementary material, which is available to authorized users.

✉ Susan E. Hough
hough@usgs.gov

Stacey S. Martin
7point1@gmail.com

Vineet Gahalaut
vkgahalaut@yahoo.com

Anand Joshi
anandfes@iitr.ernet.in

R. Bossu
bossu@emsc-csem.org

¹ United States Geological Survey (USGS), Pasadena, 525 South Wilson Avenue, Pasadena, CA 91106, USA

² Earth Observatory of Singapore (EOS), Nanyang Technological University, 50 Nanyang Avenue, N2-01a-14, Singapore 639798, Singapore

³ National Centre for Seismology (NCS), Delhi, Ministry of Earth Sciences, Lodhi Road, New Delhi 110003, India

⁴ Department of Earth Sciences, Indian Institute of Technology (IIT) Roorkee, Roorkee 247667, India

⁵ European-Mediterranean Seismic Centre, c/o Commissariat à l’Energie Atomique Centre DAM Ile de France, 91297 Arpajon CEDEX, France

consistent with the Atkinson and Boore (Bull Seism Soc Am 93:1703–1729, 2003) subduction zone ground motion prediction equation (GMPE). At greater distances ($R_{RUP} > 200$ km), instrumental PGA values are consistent with this GMPE, while PGA_{EMS} is systematically higher. We suggest the latter reflects a duration effect whereby effects of weak shaking are enhanced by long-duration and/or long-period ground motions from a large event at regional distances. We use PGA_{EMS} values within 200 km to investigate the variability of high-frequency ground motions using the Atkinson and Boore (Bull Seism Soc Am 93:1703–1729, 2003) GMPE as a baseline. Across the near-field region, PGA_{EMS} is higher by a factor of 2.0–2.5 towards the northern, down-dip edge of the rupture compared to the near-field region nearer to the southern, up-dip edge of the rupture. Inferred deamplification in the deepest part of the Kathmandu valley supports the conclusion that former lake-bed sediments experienced a pervasive nonlinear response during the mainshock (Dixit et al. in *Seismol Res Lett* 86(6):1533–1539, 2015; Rajaure et al. in *Tectonophysics*, 2016). Ground motions were significantly amplified in the southern Gangetic basin, but were relatively low in the northern basin. The overall distribution of ground motions and damage during the Gorkha earthquake thus reflects a combination of complex source, path, and site effects. We also present a macroseismic intensity data set and analysis of ground motions for the M_w 7.3 Dolakha aftershock on 12 May 2015, which we compare to the Gorkha mainshock and conclude was likely a high stress-drop event.

Keywords Gorkha · Nepal · Earthquake · Ground motions

1 Introduction

The widespread reach of the macroseismic shaking effects from earthquakes in Nepal and regions along the Himalayan frontal arc were recognized in ancient times by medieval Indian scholars (e.g. Iyengar 1999). In the Indian Subcontinent, chronological compilations of historical earthquakes utilize spatial distributions of shaking effects collated from documentary evidence (e.g. Smith-Baird 1844; Oldham 1883), and contemporary investigators have used these to estimate macroseismic intensities and magnitudes for selected events (e.g. Bilham 1999; Ambraseys and Douglas 2004; Martin and Szeliga 2010; Szeliga et al. 2010). A growing number of completed and ongoing palaeoseismic studies in the Nepal Himalayas (Lavé et al. 2005; Mugnier et al. 2005; Sapkota et al. 2013; Bollinger et al. 2014; Murphy et al. 2014; Karakaş et al. 2015; Bollinger et al. 2016; Hossler et al. 2016) have contributed further to our knowledge of pre-instrumental earthquakes in the region, although the catalogue clearly remains far from complete. It is clear that Himalayan earthquakes pose a significant hazard to not only Nepal and the Kathmandu valley specifically, but also the densely populated and rapidly urbanizing Gangetic Basin (e.g. Hough and Bilham 2008). Being the largest known earthquakes in the central Himalayas in nearly two centuries, the observed and recorded ground motions generated by the M_w 7.8 Gorkha and M_w 7.3 Dolakha earthquakes in Nepal are crucial to understand the potential impact of future earthquakes and to improve our characterization of historical events.

The Gorkha mainshock on 25 April 2015 was responsible for extensive damage and heavy casualties in central Nepal, and shaking was widely felt in the Indian subcontinent where it was responsible for light damage at many locations within the geosynclinal sediments of the Gangetic basin (Martin et al. 2015). Although the earthquake took a heavy human toll, damage was unexpectedly low in the Kathmandu Valley (Martin et al. 2015) a

surprising result given the magnitude of the event, the directivity of the rupture, its proximity to population centres, and the fragility of the local building stock (Hough 2015). The largest aftershock, the M_w 7.3 Dolakha earthquake, was also a significant event in its own right, generating shaking that was widely felt throughout Nepal and in much of the northern Indian subcontinent.

Investigations of ground motions from the Gorkha and Dolakha earthquakes have been hampered by a paucity of strong motion data. Although both earthquakes were well recorded at regional and teleseismic distances (Mitra et al. 2015; Prakash et al. 2016), limited strong motion data are available for near-field and close regional distances. For the Gorkha mainshock, data from a total of six near-field strong motion instruments are available from Nepal, all from within the Kathmandu valley (Dixit et al. 2015; Bhattarai et al. 2015; Galetzka et al. 2015; Rajaure et al. 2016; Takai et al. 2016 Table 1). Data from four strong motion recordings in the Kathmandu valley were unavailable to the scientific community until recently (Takai et al. 2016), but peak accelerations and velocity values were made available to the authors in late 2015. In India, the Gorkha earthquake was recorded by 14 stations belonging to the National Strong Motion Instrumentation Network (NSMI; Kumar et al. 2015; Table 1) and 18 stations of the Central Indo-Gangetic Plains (CIGN) network (Chadha et al. 2015). In this study, we also consider available strong motion data for the Dolakha aftershock from four instruments in the Kathmandu valley (see Dixit et al. 2015) and three NSMI stations in India. Station locations from the NSMI network, along with sensor specifications and site characteristics, are given by Kumar et al. (2015).

1.1 Macroseismic data from the Gorkha and Dolakha earthquakes

To constrain the intensity distribution more fully, in the weeks following the 25 April earthquake, Martin et al. (2015) undertook an exhaustive analysis of accounts from conventional news outlets as well as social media, interpreting 1998 European Macroseismic Scale (hereinafter EMS-98) intensities at over 3000 locations following the guidelines of Grünthal (1998) and practices employed by Martin and Szeliga (2010). Following Topozada and Real (1981) and Ambraseys and Douglas (2004), landslides, rock falls, and other forms of ground failure were not considered in assignments, as they are known to occur at different ranges of intensity (Grünthal Grünthal 1998). The EMS-98 scale supersedes the Medvedev-Sponheur-Kárník or MSK scale (Medvedev et al. 1965), and different versions of both have been used in macroseismic studies in the Indian Subcontinent (e.g. Udhoji et al. 2000; Pande and Kayal 2003). The results of these and other studies were revisited using EMS-98 and were incorporated by Martin and Szeliga (2010) in their catalogue of uniformly assessed macroseismic observations from historical and modern earthquakes in the Indian subcontinent. EMS-98 is generally consistent with intensities that use the Modified Mercalli Intensity scale (MMI; Musson et al. 2010). In this study, we also use the same approach to assess intensities for the Dolakha aftershock, presenting a summary of its macroseismic effects. At the time the Dolakha event occurred, attentions remained focused on the effects of the Gorkha mainshock; this M_w 7.3 aftershock was, however, a significant earthquake in its own right.

Most of the data sources used by Martin et al. (2015) for the Gorkha mainshock and by this study for the Dolakha aftershock were derived from newspaper reports, which are a faithful resource regularly tapped to study historical earthquakes in the Indian Subcontinent and in other parts of the world (e.g. Martin and Szeliga 2010; Martin and Hough 2015). A known caveat (e.g. Topozada and Real 1981; Hough and Pande 2007) regarding written earthquake accounts, including newspaper accounts, is the tendency to focus on

Table 1 Recorded PGA and PGV values for the 25 April 2015 Gorkha earthquake

Location	Station Code	Latitude (N)	Longitude (E)	R _{RUP} (km)	PGAx	PGAy	PGAz	PGVx	PGVy	PGVz
Phulchowk	PTN	27.681	85.319	13.1	0.154	0.136	0.151	74	72	64
Bhaktapur	THM	27.713	85.377	13.5	0.150	0.124	0.183	90	90	64
Kirtipur	KTP	27.682	85.273	13.7	0.153	0.246	0.123	52	30	46
Tribhuvan University	TVU	27.681	85.288	13.6	0.192	0.242	0.150	99	83	51
Kanti Path	KAT	27.713	85.316	14.1	0.150	0.165	0.186	107.3	86.0	58.8
Lainchaur	DMG	27.719	85.317	14.4	0.178	0.127	0.206			
Bahaga	BAG	27.134	84.060	121.5	0.049	0.059	0.047	7.417	8.569	2.825
Motihari	MTR	26.631	84.899	129.2	0.081	0.082	0.034	9.250	7.375	3.627
Darbhangga	DRB	26.117	85.900	152.5	0.073	0.076	0.036	10.613	9.265	2.967
Maharajganj	MAH	27.141	83.537	161.3	0.068	0.052	0.017	11.297	6.773	2.174
Patna	PTN	25.622	85.149	228.3	0.034	0.047	0.026	3.398	4.379	1.864
Kishanganj	KSN	26.095	87.948	248.7	0.035	0.041	0.019	11.669	11.808	3.452
Utraula	UTR	27.310	82.415	252.6	0.034	0.041	0.018	3.041	4.160	1.484
Jaunpur	JAU	25.736	82.693	338.1	0.020	0.022	0.013	3.510	1.929	1.128
Knalichina	KNA	29.670	80.670	446.8	0.003	0.004	0.005	0.433	0.540	0.585
Askote	ASK	29.760	80.330	482.9	0.008	0.008	0.008	0.380	0.935	0.664
Pitoragath	PIT	29.580	80.210	487.1	0.006	0.010	0.012	0.466	1.045	0.769
Bageshwar	BHA	29.830	79.770	539.1	0.003	0.004	0.005	0.405	0.391	0.477
Berimag	BER	29.770	80.050	509.9	0.002	0.002	0.003	0.437	0.502	0.698
Kamadevi	KAM	29.840	79.960	521.4	0.002	0.003	0.003	0.392	0.551	0.465
Kapkote	KAP	29.940	79.890	532.2	0.004	0.005	0.006	0.341	0.408	0.505

dramatic effects, often without indication of the prevalence of these effects in the immediate vicinity. Additionally, as noted by Martin and Kakar (2012) and Martin and Hough (2016), increased societal awareness of earthquakes, sociocultural responses, and an economically driven change in the built-up environment in the Indian subcontinent tends to result in inflation of intensity assignments at lower levels of shaking if the EMS-98 guidelines are followed too stringently. These issues are addressed here and in Martin et al. (2015), for example by incorporating the approach of Martin and Kakar (2012) for EMS-98 levels 2–5, an approach similar to that taken by Topozada and Real (1981) and incorporated by other studies (e.g. Meltzner and Wald 1998, 2002).

The EMS-98 scale includes extensive supporting materials and guidelines to distinguish between the severity (grades) of damage to different construction types by using vulnerability classes (Grünthal 1998) when these are available. This aspect of the scale was critical to reliably assess intensities because apparently catastrophic damage (i.e. complete collapse equivalent to Grade 5) of vulnerable masonry buildings tends to saturate above MSK VII–VIII (Ambraseys and Douglas 2004) equivalent to 7–8 EMS given the prevalent building types in the mountainous regions of Nepal (e.g. mud-bonded brick or stone masonry; Chaulagain et al. 2015). Shaking severity of 8 EMS, for example, corresponds to widespread moderate damage to reinforced cement concrete buildings without earthquake resistant design. As discussed in more detail in the following section, the availability of detailed EMS-98 guidelines, applied based on experiences with earthquakes in the Indian subcontinent, is critical to avoid inflated intensities for locations where heavy damage is experienced, but virtually all structures are very weak.

It is also difficult, at times impossible, to estimate the health of a structure, its construction type, building materials and the practices employed during construction from newspaper sources. To counter this impediment, singular reports of the collapse of *kaccha* (makeshift construction using branches, bamboo, wood, mud, etc.) walls, parapets, or balconies were assigned 5–6 EMS, whereas the collapse of *pakka* (typically stone or brick) walls or roofs were assigned 6 EMS. These adjustments prevent inflation of intensities in the absence of statistical quantities while also providing ranges as recommended by Grünthal (1998) for historical data derived from similar sources. Rigorous application of the EMS-98 scale requires information about the prevalence of effects that could be gleaned from ground-based surveys, but is almost never available from documentary, non-technical sources such as newspapers. Ground-based surveys would, however, clearly be impractical for an earthquake as widely felt as the Gorkha event. Moreover, intensity assessments based on written sources provide a better basis of comparison with historical earthquakes, for which detailed, scientific ground surveys are rarely available. A media-based intensity assessment can thus provide a better basis for comparison for analysis of historical earthquakes.

The final intensity data set included accounts from 3831 locations for the Gorkha mainshock (Martin et al. 2015; Fig. 1) and 1100 locations for the Dolakha aftershock (this study; electronic supplement; Fig. 2) for which there were both reliable geographic coordinates and sufficient information to assess intensities or to document that shaking was felt. Of the total, intensity values are assessed for 3155 and 920 locations for the Gorkha and Dolakha events, respectively. Each intensity value was assigned a subjective quality rating following Musson (1998). These data sets provide the only spatially rich available information that can be used to investigate the near-field and regional distribution of mainshock ground motions (e.g. Dixit et al. 2015; Ampuero et al. 2016).

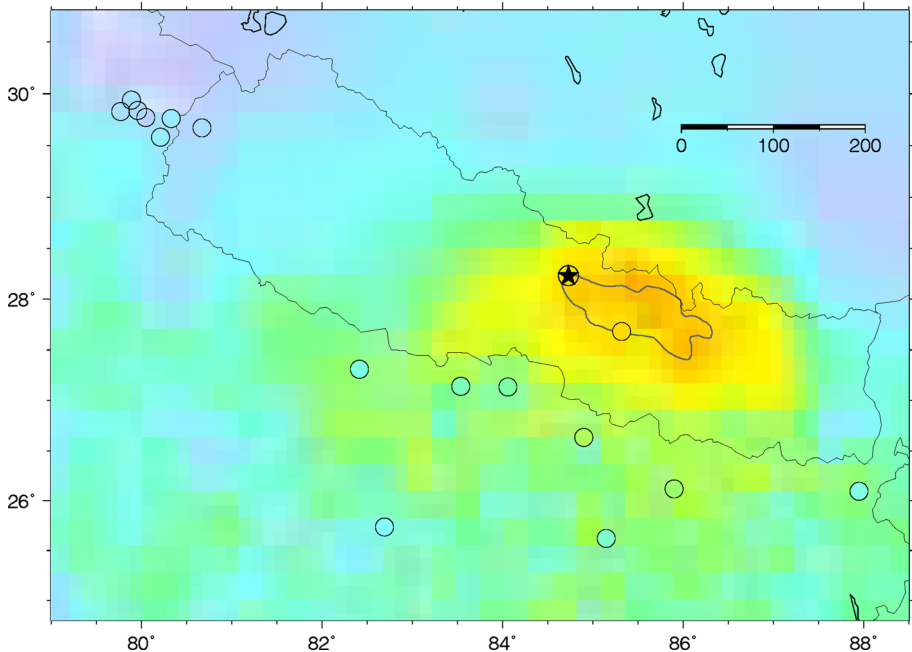


Fig. 1 Intensity data (contoured using same colour scale as shown in Fig. 2) from Martin et al. (2015) for the Gorkha mainshock, and inferred EMS-98 intensity values using PGA–intensity relationship from Worden et al. (2012) to convert recorded PGA values at strong motion sites (*filled circles*). National borders and mainshock rupture perimeter from Lindsey et al. (2015) are also indicated (*light and dark lines*, respectively). *Star* indicates mainshock epicentre

1.2 Validation of Martin et al. (2015) intensities

The intensity data set published by Martin et al. (2015) was questioned by Tertulliani et al. (2016), who argued that both near- and far-field intensity assignments were too low. Martin and Hough (2016) presented a detailed reply to this comment. Since the Martin et al. (2015) results provide the foundation for this study, here we further consider two independent data sets that have become available since Martin et al. (2015) and Martin and Hough (2016) were published: detailed damage survey results for the village of Sankhu (27.728 N, 85.469E) located east of central Kathmandu (Ohsumi et al. 2016), and independently derived, automated EMS-98 intensity assignments from the European-Mediterranean Seismological Centre (EMSC). The latter are presented in detail by the companion paper (Bossu et al. 2016), with results described briefly here.

Following the Gorkha earthquake, the National Research Institute for Earth Science and Disaster Prevention (NIED) dispatched several field survey teams to the affected area (Ohsumi et al. 2016). Of note for this study, one of the teams surveyed the degree of damage for every house in the village of Sankhu using the EMS-98 scale, with separate damage statistics compiled for reinforced concrete (RC), brick with cement or lime mortar (BC), well-built mud-brick (BM-W), and poorly built mud-brick (BM) houses. Following EMS-98 guidelines, ordinary RC buildings are generally vulnerability Class C, with a range from A to as high as D depending on construction quality and other factors. Brick buildings lacking reinforcement or confinement are vulnerability Class A-B. We assume

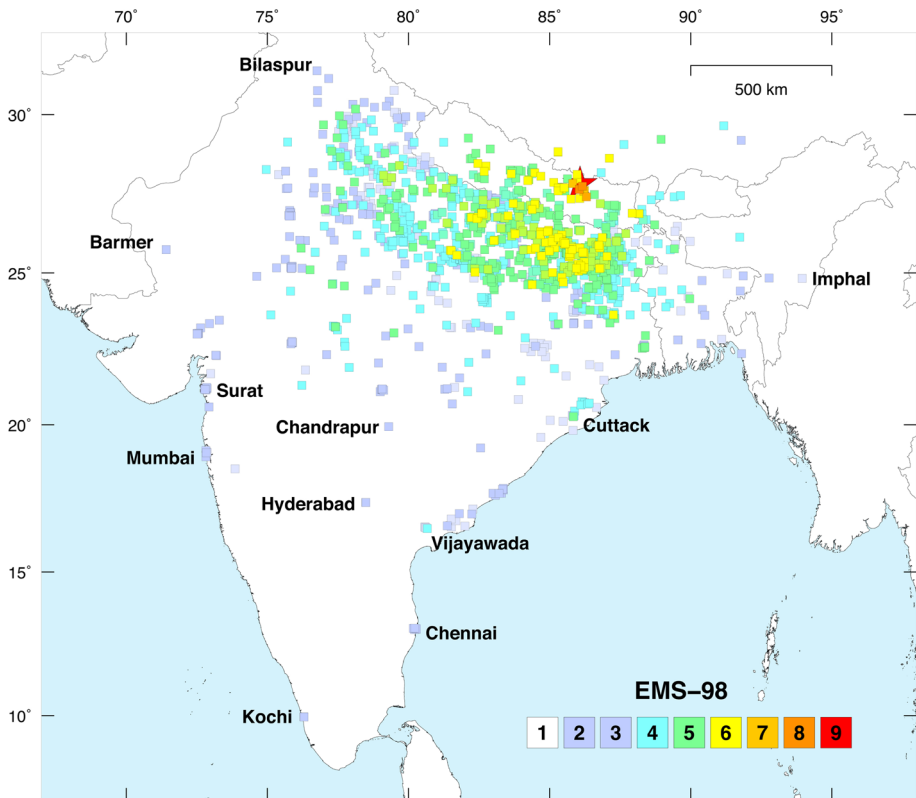


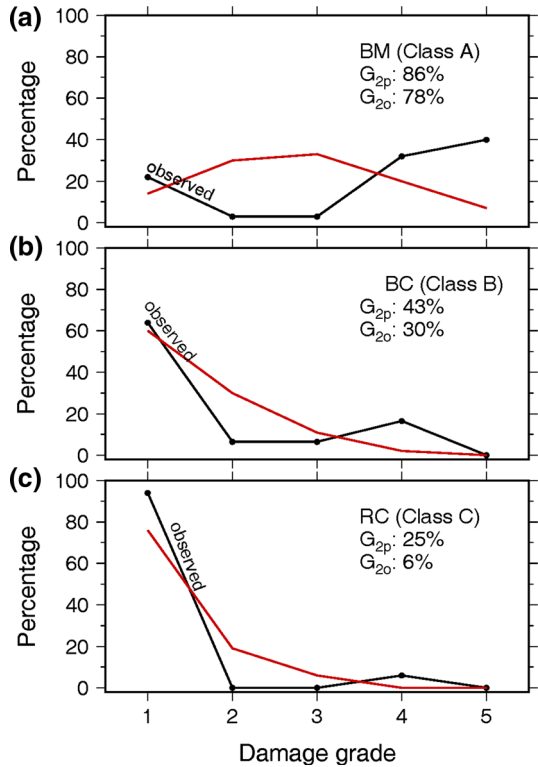
Fig. 2 EMS intensities for the 12 May 2015 $M_w7.3$ Dolakha earthquake. Epicentral location indicated by a red star

that the most vulnerable structures (BM) were Class A, while the other two Classes (BM-W, BC) were Class B.

The results of the detailed damage survey (Ohsumi et al. 2016) are shown in Fig. 3 along with expected damage for 8 EMS shaking given the definitions provided by (Grünthal 1998); these definitions include terms such as “few”, “many”, and “most” for which approximately numerical ranges are specified: few = 8 % (0–15 %), many = 35 % (15–55 %), and most = 75 % (55–95 %). The EMS guidelines (Grünthal 1998) do not include complete specifications for the expected percentages of expected damage of all grades. To estimate numerical percentages (fragility curves), we use the fragility curves inferred for Italy by Zuccaro et al. (2012).

The survey results of Ohsumi et al. (2016; Fig. 3) indicate 94 % of Class C structures were assessed to have Grade 1 damage: negligible to slight damage. As no houses of any class were deemed to have no (Grade 0) damage; we assume that Ohsumi et al. (2016) structures with no visible damage were included with Grade 1. Few (6 %) Class C structures suffered Grade 4 damage, i.e. heavy structural damage. Most (64 %) Grade B structures experienced Grade 1 damage; of the remaining 36 %, BC houses experienced more severe damage (32 % Grades 4 or 5) than did BM-W houses (22 % Grades 2–3, 14 % Grade 4). Most (72 %) of Class A structures experienced Grade 4 or 5 damage, with 22 % experiencing Grade 1 damage. The comparison of observed versus expected 8 EMS

Fig. 3 Expected EMS 8 damage (red lines Grunthal (1998) and Zuccaro et al. (2012)) versus observed damage from Gorkha mainshock (black lines Martin et al. (2015)) in the village of Sankhu, for Class A (top), B (middle), and C houses (bottom). G_{2p} and G_{2o} indicate predicted and observed percentages of Grade 2–5 damage for each building class



damage reveals that more Class A houses experienced severe (Grade 4/5) damage (72 %) than expected (26 %). In contrast, at 8 EMS ≈ 43 % of Class B structures are expected to experience Grade 2 or higher damage, compared to an observed total of ≈ 30 % for BC and BM-W houses. At 8 EMS, ≈ 25 % of Class C structures are expected to experience Grade 2 or higher damage, compared to an observed total of 6 %.

The results presented in Fig. 3 reveal that, while the most vulnerable houses sustained severe damage, even relatively vulnerable better-built (Class B and C) structures performed better than predicted for 8 EMS shaking. Direct experience with vernacular structures in Nepal suggests that, due to age and resource limitations, the oldest and weakest mud-brick houses are even more vulnerable than the typical Class A structures found in Europe and elsewhere. These results illustrate the conclusion reached by extensive earlier investigations of earthquakes in the Indian subcontinent that the MSK scale (the predecessor of the EMS-98 scale) saturates at MSK VII–VIII in many regions due to the prevalence of extremely weak buildings (e.g. Ambraseys and Bilham 2003a, b; Ambraseys and Douglas 2004). In effect, damage to better-built structures, even when they are relatively weak, provides a more reliable indication of overall shaking severity. In the case of Sankhu, the detailed damage survey does not support EMS-98 intensity as high as 8. Based largely on field visits (Roger Bilham, written comm. 2015), Martin et al. (2015) assigned 7–8 EMS for the western part of Sankhu and 6–7 EMS for the eastern part of the village, which was less heavily damaged.

We also consider the intensity data set obtained from the EMSC on-line system, which are determined using an algorithm from responses to on-line questionnaires. A full

description of this system, and its recent adaptations to capture the increasingly high percentage of responses submitted from Smartphones rather than traditional computers, is provided by the companion paper (Bossu et al. 2016). Key results for this study are presented in Fig. 4, which compares Martin et al. (2015) intensities with automated EMS-98 intensities from the EMSC. Available “Did You Feel It?” (DYFI; Wald et al. 1999) (modified Mercalli) intensities are also shown. As illustrated by Fig. 4, mean Martin et al. (2015) intensities and EMSC intensities are consistent, with both data sets characterized by a smooth decay of mean values. Both sets of results are also consistent with available DYFI data, although these data reveal more scatter at distances within 200 km. Considering individual intensities, sparse EMSC and DYFI values for distances within 100 km are generally consistent with the range of individual intensities assigned by Martin et al. (2015). Both EMSC and DYFI data include more high as well as low outliers, for example with values as high as 10 and as low as 2 for distances of 80–100 km. Such extreme values were not supported by any written accounts, suggesting that, compared to a thorough consideration of media sources, automated on-line systems generate more spurious values. In summary, while intensity values are inherently subjective and uncertain to some extent,

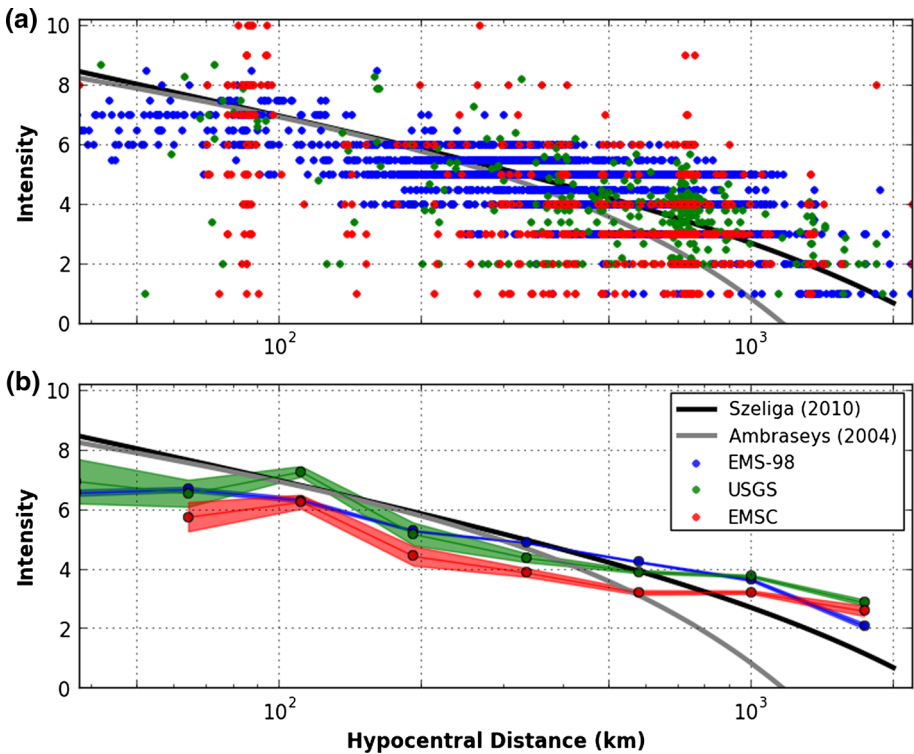


Fig. 4 **a** (top panel). Individual Gorkha mainshock intensity assignments from Martin et al. (2015) (blue dots), EMSC system (Bossu et al. (2016); red dots), and DYFI system (Wald et al. (1999); green dots). **b** (bottom panel). Bin-averaged mean values for the same data sets. Shading indicates ± 1 standard deviation of the mean calculated for (logarithmic) distance bins. Black and grey lines show intensity prediction equations from Szeliga et al. (2010) and Ambraseys and Douglas (2004), respectively. (The Ambraseys and Douglas (2004) equation is developed using intensity data up to ≈ 1200 km)

available independent data and observations offer further validation of the Martin et al. (2015) intensity assignments.

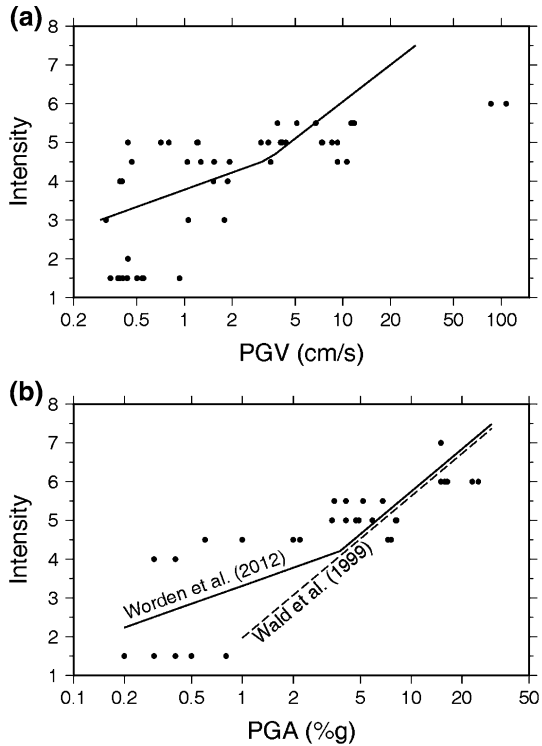
1.3 Comparison of PGA and PGV versus observed macroseismic intensity

To fully exploit these macroseismic data and thereby investigate ground motions, it is necessary to convert EMS-98 values to an estimated instrumental ground motion measure such as peak ground acceleration (PGA) or peak ground velocity (PGV). Relationships between PGA and PGV as a function of macroseismic intensity have been developed from data in southern California, using intensity data determined with the MMI scale (e.g. Wald et al. 1999; Worden et al. 2012). Given the close correspondence between EMS-98 and MMI intensities (Musson et al. 2010), one expects the published relationships to hold for EMS-98 intensities as well. It is possible that the relationship between instrumental PGA and intensity will be regionally variable, as inferred by Caprio et al. (2015); it is also possible that an incomplete consideration of differences in vulnerability will give rise to an apparent regional variation in the relationship.

Since 1999, sparse instrumental data for damaging earthquakes in the USA have been supplemented with intensity data from the USGS Community Internet Intensity Map (CIIM) system (also known as “Did You Feel It?” DYFI; Wald et al. 1999). Consistently interpreted, spatially rich DYFI intensity data are used routinely to improve ShakeMap representations (Worden et al. 2010) and to investigate ground motions (e.g. Hauksson et al. 2008; Hough 2012). Outside the USA and its territories, however, the DYFI system has limitations (Martin and Hough 2015, 2016; Martin et al. 2015); data are often sparse, with intensities determined without consideration of building types and vulnerability, or can be skewed by sociocultural factors.

The Martin et al. (2015) and DYFI intensities should be generally consistent, but they are determined using different scales (EMS-98 versus MMI) and with subjective traditional human assessments versus objective automated, algorithm-based assessments, respectively. It is also possible that as noted earlier, the fundamental relationship between intensity and PGA might be regionally variable. We therefore first compare the intensity data with instrumentally recorded ground motions to test the validity of published relationships for the Gorkha earthquake. For this study, we collect a total of 21 available strong motion recordings from India and Nepal (Table 1) to test the validity of previously published PGA–intensity relations. Full-waveform data are available for some of the stations; for others, only limited peak acceleration and/or velocity information has been made available. Using information available to date, we compare instrumental peak acceleration and peak velocity (PGA, PGV) with the intensity from the location closest to the instrumental recording site. To estimate PGV from strong motion data, we high-pass-filter the records above 0.1 Hz. For all but two stations, the nearest intensity is within 10 km; for the remaining two stations, the nearest intensity values are 17 and 25 km away. Given that ground motions can vary significantly over even short distances, the scatter evident in Fig. 5 is not surprising. For PGA values above approximately 1 %g, the results are nonetheless well fit by the Worden et al. (2012) relationship between PGA and intensity, developed using data from earthquakes in southern California (Fig. 5). We use the Worden et al. (2012) relationships that do not include magnitude and distance dependence, which is found to fit the observed data well on average. For PGA below approximately 1 %g, Fig. 5b suggests that shaking can be barely felt (1–2 EMS) or felt at a higher (4 EMS) level (the lack of 3 EMS values is likely a consequence of the small sample size). As a speculation, we suggest that very weak, long-period shaking from large earthquakes at regional

Fig. 5 a (top). Instrumentally recorded PGV values for the Gorkha mainshock versus Martin et al. (2015) EMS values from the location closest to each instrument, and PGV–intensity relationship from Worden et al. (2012) (black line); **b (bottom)** Instrumentally recorded PGA values versus Martin et al. (2015) EMS value from the location closest to each instrument. Dashed line indicates relationship from Wald et al. (1999); solid line indicates relationship from Worden et al. (2012)

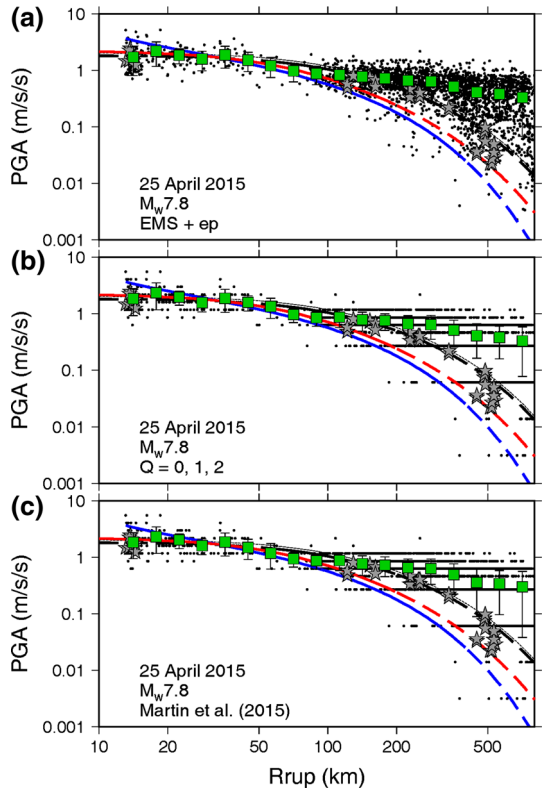


distances will have markedly different macroseismic effects depending on the nature of local structures. On average, however, the Worden et al. (2012) relationship still fits the data well.

We therefore use the Worden et al. (2012) relationship without modification to estimate PGA_{EMS} values from the Martin et al. (2015) intensity data (Fig. 6). To analyse the results, we will not focus on the absolute PGA_{EMS} values but rather on the distribution of residuals relative to a baseline. Residuals can be estimated relative to an average curve fit through the data set, as was done by Hough (2012) for DYFI intensities for the 2011 Mineral, Virginia earthquake. For this study, we instead consider published ground motion prediction equations (GMPEs). Chadha et al. (2015) showed that instrumentally recorded PGA values at all distances are consistent with the Atkinson and Boore (2003a, b; hereinafter AB03) subduction zone GMPE, developed for the distance range 50–300 km. This GMPE, with $M_w 7.8$ and National Earthquake Hazards Reduction Program (NEHRP) site Class C/D (very dense soil and soft rock/stiff soil), fits instrumentally recorded PGA values analysed in this study as well as PGA_{EMS} values for R_{RUP} within ≈ 200 km (Fig. 4). We note that although this GMPE was developed for nearest-fault distances greater than 50 km to avoid near-source saturation effects, it provides a good fit to available near-field PGAs for the Gorkha mainshock. This Ground Motion Prediction Equation (GMPE) is also consistent with available instrumental data from all distances.

Rajaure et al. (2016) compared data in the Kathmandu Valley to the GMPE developed under the Next-Generation Attenuation project (Boore et al. 2014; hereinafter BSSA14) and concluded that this relationship is more consistent than the AB03 relationship with observed long-period spectra in the Kathmandu valley. The BSSA14 GMPEs are based on

Fig. 6 Instrumental Gorkha mainshock PGA values (grey stars) and estimated PGA_{EMS} values (black circles) as a function of nearest-fault distance. Bin-averaged PGA_{EMS} values also shown (green squares). Black lines indicate predicted PGA using Atkinson and Boore (2003) GMPE for NEHRP Site Classes C (dark line) and D (lighter line), assuming $M_w 7.8$. Blue line indicates predicted PGA using Boore et al. (2014) GMPE, converting nearest distance to surface projection of fault (R_{jb}) to R_{rup} . Red line indicates predicted PGA using Ghofrani and Atkinson (2014) GMPE. Panels a, b, and c show, respectively, all intensities, intensities with quality factors 0, 1, and 2, and intensities plus random uncertainties. Dashed lines indicate extrapolations of GMPE beyond distance range for which each is constrained



the Joyner-Boore distance, defined as the nearest distance from any point to the surface projection of the fault, and are developed for Joyner-Boore distances of 0–400 km. The BSSA14 PGA relationship also fits the instrumental PGA data and PGA_{EMS} estimates reasonably well for R_{RUP} less than 100 km, with somewhat higher values for distances less than about 20 km, but significantly less well than does AB03 at greater distances (Fig. 6). A third published GMPE (Ghofrani and Atkinson 2014), developed for nearest-fault distances up to 200 km, also fits the instrumental and PGA_{EMS} results less well than does AB03. These comparisons reveal that no single published GMPE provides a good fit to Gorkha ground motions at all frequencies of engineering concern. This result is not surprising: large Himalayan megathrust earthquakes might be characterized by similar source properties as subduction zone earthquakes, but in a different tectonic setting that is likely to have different attenuation. Development of a new GMPE that incorporates Gorkha and Dolakha data is beyond the scope of this study. Rather than focusing on absolute shaking levels, we therefore focus on residuals for R_{RUP} within 200 km, using AB03 as the best available baseline.

At distances greater than 200 km, three factors (in addition to possible site response) might contribute to the discrepancy between estimated and predicted values: (1) as mentioned, relatively high intensities at regional distances might be generated in some cases by long-period, low-PGA shaking (for example, regional ground motions with 2-s period might be felt strongly in mid-rise buildings); (2) at progressively large distances, shaking is more likely to be reported only at locations associated with high local amplifications, such

that an instrumental recording is less likely to reflect the nearest reported intensity; and (3) even in the absence of long-period effects, at large distances, shaking with low PGA but long durations due to scattered waves and/or converted surface waves will generate stronger effects than short-duration shaking with the same PGA (Szeliga et al. 2010). The discrepancy between estimated PGA_{EMS} values and both GMPEs is nearly two orders of magnitude at the largest distances, which cannot be plausibly explained as a consequence of site effects and reporting biases alone. We therefore conclude that the discrepancy is at least in part a consequence of duration and/or long-period effects, with reporting biases likely contributing to some extent as well. These effects are difficult to separate. We further note that both the AB03 relationship and the Ghofrani and Atkinson (2014) GMPE are valid only for distances up to 200 km. In the following sections, we therefore focus on analysis of ground motions within 200 km. While shaking levels at distances greater than 200 km are generally of a lesser concern for hazard, dramatic counter-examples such as damage in Mexico City from the 1985 M_W 8.1 Michoacán earthquake (Singh et al. 1988) illustrate the importance of characterizing ground motions at regional distances.

While PGA_{EMS} residuals within nearest-fault distances of 200 km are considered reliable, they are still characterized by uncertainties due to multiple factors, including: 1) the choice of baseline, 2) the inherent uncertainty of any GMPE, 3) the inherent subjectivity and imprecision of EMS assignments, and 4) the EMS–PGA conversion. For example, the AB03 GMPE itself is characterized by a log-base-10 standard deviation of 0.23, which corresponds to a one-sigma uncertainty of a factor of ≈ 1.7 . The EMS–PGA relationship of Worden et al. (2012) has a log-base-10 uncertainty of 0.39, corresponding to a one-sigma uncertainty of ≈ 2.5 . A formal consideration of total uncertainty suggests that none of the observed systematics in the distribution of residuals is statistically significant. Based on our direct experiences, including both ground-based surveys of the Kathmandu valley and exhaustive consideration of media reports, as well as published reports by other authors (e. g. Hashash et al. 2015), this conclusion is overly pessimistic. For example, damage in the central Kathmandu valley was remarkably low, while damage was still low but generally more severe around the edges of the valley (Hashash et al. 2015; Martin et al. 2015). To explore the robustness of our results, in the following sections we will also consider (1) residuals relative to the BSSA14 PGA GMPE, (2) residuals relative to AB03 using only Martin et al. (2015) intensities with qualify factors 0, 1, and 2, and (3) residuals calculated from Martin et al. (2015) intensities plus or minus a random ε between -0.5 and 0.5 .

1.4 Near-field ground motions

Martin et al. (2015) showed that near-field shaking was lower than expected given the Szeliga et al. (2010) Himalaya model, which was developed for distances up to 2000 km (Fig. 4). To further consider the variability of near-field ground motions for the Gorkha event, we consider PGA amplification across the near-field region relative to PGA predicted using the AB03 subduction zone GMPE assuming M_W 7.8 and NEHRP Class C, which, as discussed above, provides the best overall fit to instrumental PGA data. (As illustrated by Fig. 4, predictions for site Classes C and D are nearly indistinguishable.) The resulting near-field amplification map is shown in Fig. 7a, which also indicates the surface projection of the rupture from Lindsey et al. (2015). Note that, due to the nearly flat mainshock fault geometry, R_{RUP} is nearly constant over the near-field region. The resulting amplification map reveals that relatively stronger ground motions were concentrated along the northern edge of the rupture, above the down-dip rupture edge. Considering the observed EMS-98 intensity distribution from the 25 April mainshock, Ampuero et al.

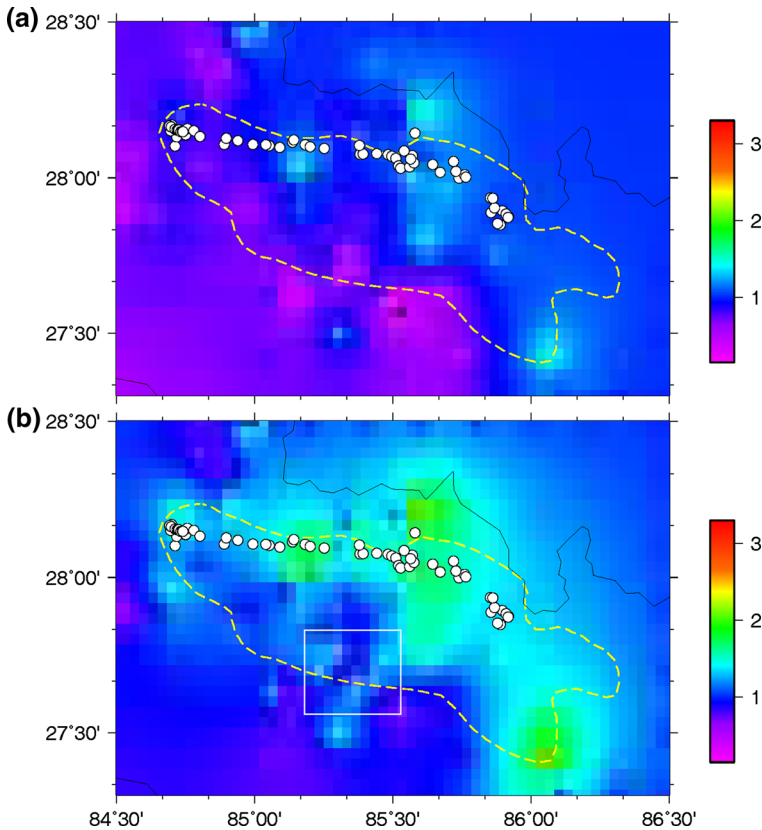


Fig. 7 **a** (top). PGA_{EMS} amplification across the near-field region relative to the BSSA14 GMPE using Gorkha mainshock data. Filled white circles indicate locations of high-frequency radiation as estimated from back-projection analysis Ampuero et al. (2016). Border with Tibet and perimeter of rupture Lindsey et al. (2015) are also shown (light black and dashed light lines, respectively). **b** (bottom). Residuals relative to Atkinson and Boore (2003) GMPE, assuming M_w 7.8 and NEHRP Class C. High-frequency sources and rupture perimeter again shown. White box indicates location of Fig. 8

(2016) showed that higher intensities correlate with the predominant sources of high-frequency radiation, which were concentrated along the down-dip rupture edge (also see Avouac et al. 2015; Meng et al. 2016). Our PGA_{EMS} amplification map (Fig. 7a) is based almost entirely on observed intensities across the near-field region, so it reveals essentially the same spatial pattern with more quantitative estimates of amplification factors. In proximity to high-frequency sources, amplification of PGA_{EMS} is generally a factor of 2–3. If residuals are calculated relative to the BSSA14 PGA_{EMS} (Fig. 7b), residuals are generally lower, but characterized by the same north-to-south trends, with a similar relative amplification of PGA_{EMS} values towards the northern edge of the rupture.

Focusing on the Kathmandu valley, observed intensities reveal lower damage in the central, deepest part of the valley during the 25 April mainshock (Fig. 8; Martin et al. 2015). PGA_{EMS} amplification relative to AB03 again reveals the same distribution (Fig. 8b), with deamplification of a factor of, typically, 10–40 % at most locations in the central valley. While shaking is generally consistent with the AB03 relationship (i.e. amplification of 1.0) at foothill sites adjacent to the valley, locally high amplifications,

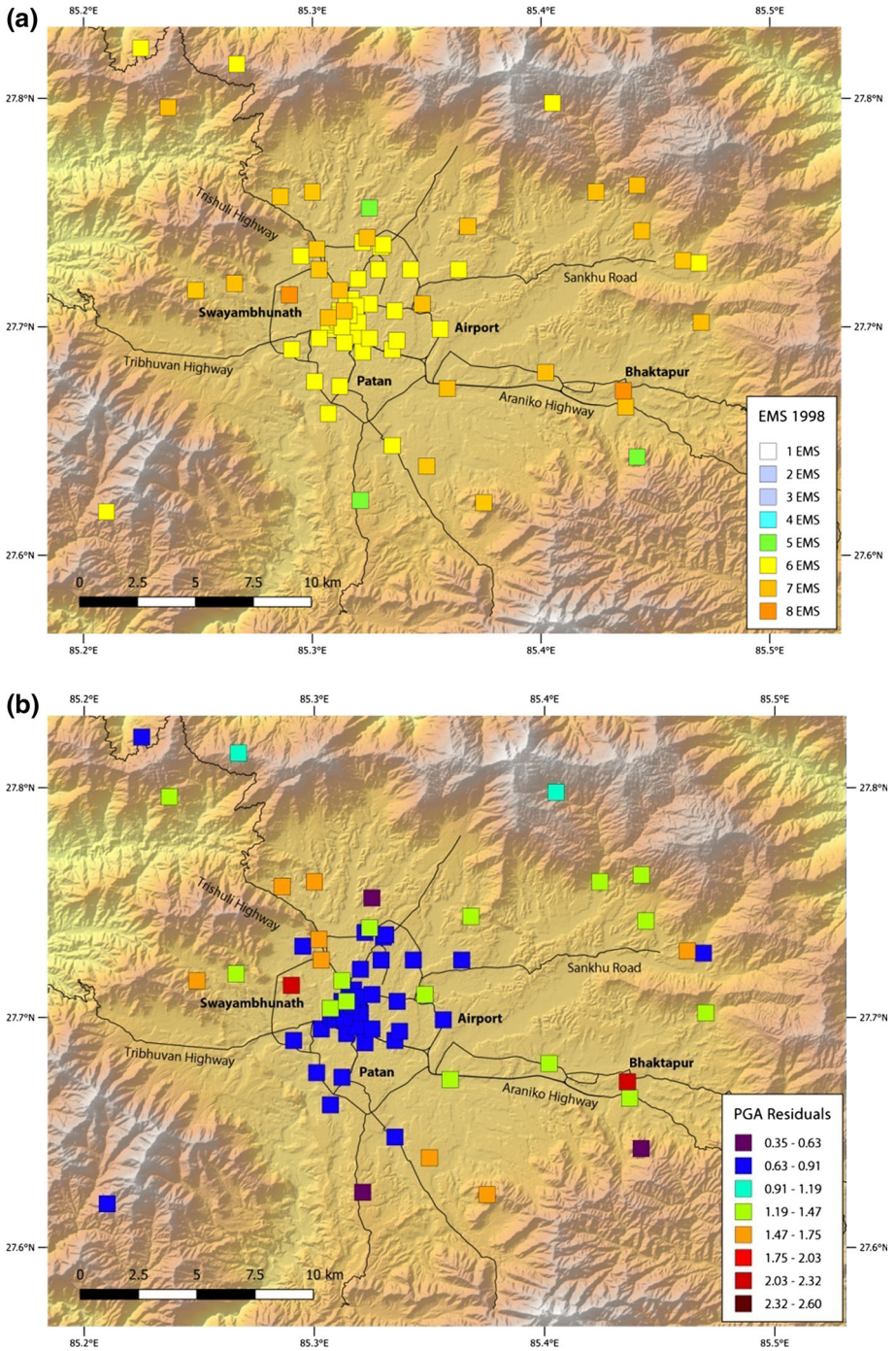


Fig. 8 **a** (top). Close-up of EMS intensities across the Kathmandu Valley from the Gorkha mainshock; **b** (bottom) PGA residuals (amplification or deamplification) relative to AB03 GMPE

reaching a factor of 1.5–2.0, are inferred at a number of sites including at the Swayambunath Temple, in Sankhu, and in parts of Bhaktapur, all of which are attributed to topographic amplification effects.

PGA_{EMS} amplification/deamplification estimated from intensities for valley versus foothill sites can be compared with soil-to-rock amplification/deamplification estimated from instrumental data (Rajaure et al. 2016). The results are consistent: 0.63–0.91 for 40 of 66 PGA_{EMS} values at valley sites versus 0.60–0.92 for PGA (Rajaure et al. 2016). Again the factors correspond to significant variability of shaking intensities and damage. The consistency of these results provides a further measure of validation of both the intensity assignments of Martin et al. (2015) and the use of the Worden et al. (2012) relationship to estimate PGA_{EMS} .

1.5 Ground motions south of the rupture

To consider PGA_{EMS} amplification at close regional distances, we again calculate amplification factors relative to AB03 at all locations for which intensities are available (Fig. 9). We do not calculate residuals relative to BSSA14 because of the clear misfit between this PGA GMPE and the instrumental data. The resulting amplification map reveals significant amplification within the southern Gangetic basin, with amplification factors as high as 3.0–4.0 and consistently at least as high as a factor of 2.0. To the immediate south of the rupture, a zone of deamplification is found, extending into the northernmost Indo-Gangetic basin. Although intensity data from southern Nepal are sparse, available data from Martin et al. (2015) suggest that the low-intensity zone extends from immediately south of the mainshock rupture to approximately the Indo-Nepal border. Low PGA_{EMS} values between a R_{RUP} range of roughly 50–100 km (relative to the Atkinson and Boore 2003) GMPE can also be seen in Fig. 6. As amplification is expected throughout this region and has been observed during past historical earthquakes (e.g. Hough and Bilham 2008), this observation suggests that shaking to the south of the mainshock was deamplified by a source effect. Given the general eastward and northward progression of the rupture (Avouac et al. 2015; Lindsey et al. 2015), we suggest that subdued shaking to the south reflects a directivity effect. We further note that, while intensities to the east and west of the rupture are relatively sparse, available data are consistent with along-strike directivity towards the east as well.

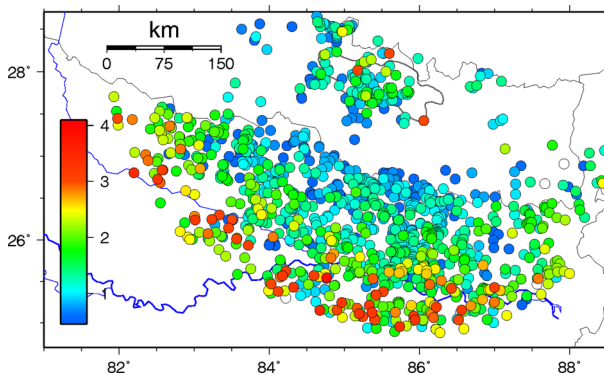


Fig. 9 Estimated PGA_{EMS} amplification relative to AB03 GMPE at regional distances from the Gorkha mainshock

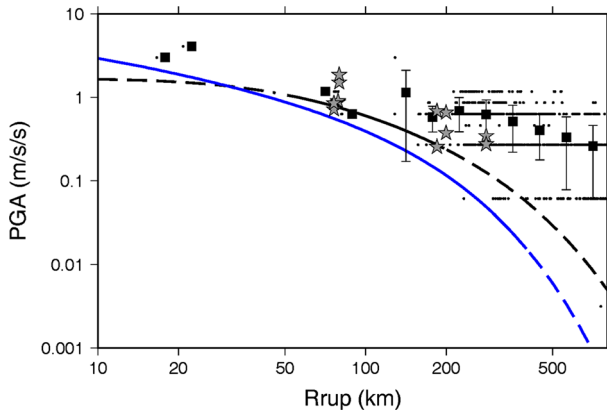


Fig. 10 Instrumental PGA values (grey stars) and estimated PGA_{EMS} values (black dots) as a function of nearest-fault (effectively hypocentral) distance. Bin-averaged PGA_{EMS} values also shown (black squares). Black line indicates predicted PGA using Atkinson and Boore (2003) GMPE for NEHRP Site Class C (dark line; dashed line indicates extrapolations) assuming $M_w7.3$. Blue line indicates predicted PGA using Boore et al. (2014) GMPE (dashed line indicates extrapolation)

1.6 Preliminary characterization of 12 May 2015 Dolakha aftershock

The $M_w7.3$ aftershock, also known as the Dolakha earthquake, on 12 May 2015 was a substantial event in its own right, with shaking that was widely felt throughout Nepal and the region. We have undertaken an investigation of the intensities of this event following the procedures used by Martin et al. (2015). Full characterization of the macroseismic effects within the meizoseismal region in Nepal is challenging due to the continued pre-occupation with the mainshock at the time the Dolakha earthquake occurred, as well as the difficulty of separating effects of the two events at locations at which damage occurred. A more complete assessment would likely require field investigation in the meizoseismal region. Nonetheless, we assign intensities at 1100 locations in the Indian subcontinent consulting digital versions of conventional newspapers and supplementing these with eyewitness accounts derived from social media, and occasionally with first-hand accounts from humanitarian aid workers on the ground. Significant damage ($7 > EMS$) and fatalities occurred in the Dolakha district, in particular in the town of Chautara where RCC-frame buildings suffered various grades of damage including total collapse (Grade 5). A few buildings damaged in the 25 April 2015 mainshock collapsed in the Kathmandu valley, e.g. at Gonagabu (eKantipur, 13 May 2015). In adjacent parts of India, the earthquake was felt in much of the Gangetic plains (Fig. 9) and damage (5–6 EMS) occurred at many places in Bihar and eastern Uttar Pradesh. Numerous, independent reports said the Dolakha aftershock was just as severe as the 25 April mainshock. The 12 May earthquake was perceived as far as Barmer (25.75 N, 71.38 E) in the west, Bilaspur (31.34 N, 76.76 E) to the north, and at Silchar (24.82 N, 92.80 E) in the east. In peninsular India, shaking rapidly diminished below 24 N latitude, south of which it was only distinctly felt in multi-storeyed buildings in cities such as Chandrapur, Mumbai, and Hyderabad. These included locations in regions underlain by Quaternary sediments such as cities in the Sabarmati basin (e.g. Ahmedabad) and in the Krishna (e.g. Vijayawada), Mahanadi (e.g. Bhubaneswar-Cuttack) and Narmada-Tapti deltas (e.g. Surat). At a distance of 2228 km, Kathrughadavu and Panampilly Nagar in Kochi (The Hindu, 13 May 2015) were the

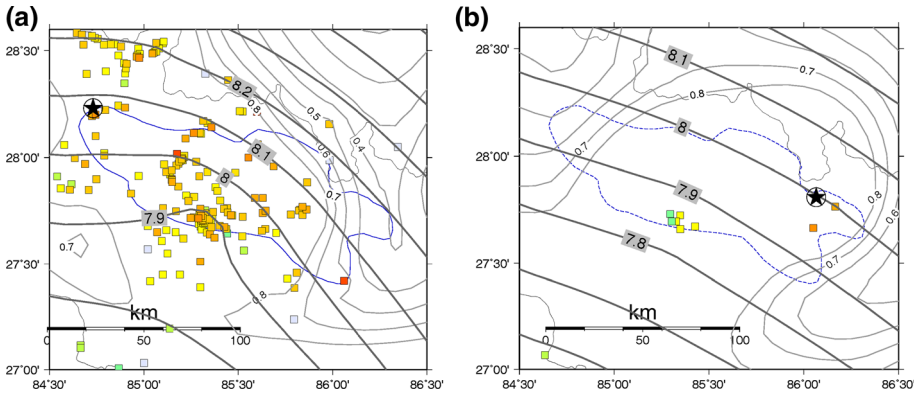


Fig. 11 **a** (left). Intensities for the Gorkha mainshock (coloured squares, same colour scale as shown in Fig. 2) are shown together with magnitudes (labelled contour lines) estimated using the Bakun and Wentworth (1997) method and the Szeliga et al. (2010) Himalaya model. Circled star indicates instrumentally determined epicentre; mainshock rupture is indicated by blue line Lindsey et al. (2015). Light lines indicate contour least-squared residuals. **b** (right) Similar result for the Dolakha event; Gorkha mainshock rupture (dashed blue line) is shown for reference

farthest locations the shock was perceived in high-rise buildings. A seismic seiche was reported in the tank at the Bhimkund temple in Madhya Pradesh (Nav Bharat, 13 May 2015) and, as in the 25 April earthquake, the water at the Bramhakund natural springs at Rajgir was discoloured again (Dainik Jagran, 13 May 2015).

For the purposes of this study, it is illuminating to consider our fairly extensive intensity data set for the Dolakha aftershock from regional distances (Fig. 2). Using EMS-98 intensities from 862 locations throughout India, we again estimate PGA_{EMS} using the Worden et al. (2012) relationship and consider available instrumental data from three stations in Kathmandu Valley (see Dixit et al. 2015) as well as three stations from the NSMI. In contrast to the mainshock, for the Dolakha aftershock, PGA and PGA_{EMS} values are generally greater than predicted by either the AB03 or BSSA14 relationship for PGA , at all distances (Fig. 10). Again, the AB03 relationship provides a better characterization of PGA decay than does BSSA14. For the Dolakha event, PGA_{EMS} within 200 km are higher than the AB03 predictions by a factor of approximately 2.0–3.0. Regardless of the EMS-to- PGA conversion, as discussed in the following section, intensities for the Dolakha event are high relative to expectations given the Szeliga et al. (2010) model. Since shaking intensities are expected to depend strongly on stress drop (e.g. Hanks and Johnston 1992; Hough 2014), this result, while preliminary, suggests that the Dolakha event was a high stress-drop event. Using results from random vibration theory, Boore (1983) shows that PGA is proportional to $\sigma^{0.8}$, where σ is stress drop. A factor of 2.0–3.0 elevation of PGA thus corresponds to a stress-drop increase (relative to the average stress drop of events used to develop the intensity prediction equation) of a factor of approximately 2.4–4.0.

1.7 Implications for historical earthquakes

The extensive intensity data sets for the Gorkha and Dolakha events will be valuable to revisit calibrations used to estimate intensity magnitudes (M_I) of historical earthquakes (e.g. Szeliga et al. 2010). While such an exercise is beyond the scope of this study, it is illuminating to consider how the recent events would have been characterized had they

occurred in historical times, assuming only the intensity data sets were available. Following the methods discussed in detail by Szeliga et al. (2010), we use the Bakun and Wentworth (1997) approach together with the Himalayan attenuation relationship developed by Szeliga et al. (2010) using the set of calibration events available at that time (Fig. 11). This approach assumes a point-source location, a known limitation of the method for analysis of events as large as the Gorkha mainshock.

For both the Gorkha and Dolakha events, near-field intensities are lower than predicted from the Szeliga et al. (2010) Himalayan model; as a result, the minimum residual solution is poorly constrained and well north of the actual locations (Fig. 11). That is, residuals are optimized when the location is pushed into a location at some distance from the near-field, in a region where intensities are unconstrained by available data. The lack of intensity data north of the events was due to a striking paucity of media accounts from Xizang (Tibet) in China. For historical earthquakes, while intensity distributions for Himalayan events are largely one-sided, some information from Xizang is generally available (e.g. Chen et al. 1982), anchoring the optimal solution to the Himalayan region. For locations plausibly close to the actual location of each events, the inferred intensity magnitude (M_I) is 7.9–8.1 for both events, i.e. reasonably close to the magnitude of the Gorkha mainshock, but overestimated significantly (0.6–0.8 units) for the Dolakha event. The latter result is again suggestive of a high stress-drop event (Hanks and Johnston 1992; Hough 2014).

These results suggest three potentially important implications for historical earthquakes. First, the fact that near-field intensities for both events are lower than expected given the Szeliga et al. (2010) Himalayan model suggests that either the near-field shaking during both events was anomalous or that near-field intensities have been systematically overestimated for both early instrumental and historical earthquakes, even when intensities are assigned following modern conservative practices (e.g. Martin and Szeliga 2010). We consider the former possibility implausible, leaving the latter as the best explanation at this stage. It will thus be important to revisit accounts of large historical Himalayan event in the light of the observations from the 2015 sequence. Second, the fact that, away from the near-field, intensities for the Gorkha mainshock are consistent with the Szeliga et al. (2010) Himalaya model suggests that the average stress drop of calibration events used to develop the model was comparable to that of the Gorkha event, but lower than that of the Dolakha event. Third, the overestimation of the intensity magnitude for the Dolakha event further illustrates the point made by Martin and Hough (Martin and Hough 2015) that magnitudes and postulated geometries of source ruptures of some historical earthquakes might be significantly overestimated or incorrect if they were high stress-drop events.

2 Conclusions

The spatially rich intensity data set for the M_w 7.8 Gorkha earthquake determined by Martin et al. (2015) provides a unique data set with which to investigate the spatial distribution of mainshock ground motions at near-field and regional distances. A comparison of instrumentally recorded PGA values with estimated PGA_{EMS} values supports the use of a published intensity–PGA relationship (Worden et al. 2012) to convert available EMS-98 data to PGA. We further note that the consistency of our results from the 25 April Gorkha earthquake with the Worden et al. (2012) relationship provides a measure of support for the reliability of the Martin et al. (2015) intensity assignments, which we also validate using two newly available independent intensity data sets. The resulting PGA_{EMS}

values provide a unique, spatially rich view of ground motions throughout the near-field region, within the Kathmandu Valley, and at regional distances in Nepal and neighbouring countries. Overall, with $R_{\text{RUP}} < 200$ km, PGA_{EMS} as well as available instrumental PGA values are consistent with the subduction zone GMPE of Aktinson and Boore (2003), assuming $M_{\text{W}}7.8$ and NEHRP site Class C. This result is consistent with the conclusions of Chadha et al. (2015) based on other regional data. The AB03 PGA relationship also provides a better fit to PGA_{EMS} values for the Dolakha event than does the BSSA14 relationship. The results of Rajaure et al. (2016) suggest, however, that long-period ground motions from the Gorkha mainshock are not consistent with the AB03 relationship.

The overall consistency of Gorkha observations with published GMPEs will thus require further investigation. It is possible that none of the published GMPEs are appropriate for the Gorkha earthquake, which may effectively have been a subduction zone source that was largely felt within a cratonic environment. For the purposes of this study, however, we conclude that the AB03 relationship for PGA provides the most appropriate baseline for estimation of amplification because this relationship best fits available instrumental (PGA) data at all distances. PGA_{EMS} amplification of a factor of 2.0–2.5 is observed throughout the near-field region even though nearest-fault distance is nearly constant. This result supports and further illuminates the conclusion of Ampuero et al. (2016) that the distribution of high-frequency energy, which was concentrated along the northern, down-dip rupture edge (Avouac et al. 2015; Meng et al. 2016), was a significant control on near-field ground motions.

Within the Kathmandu Valley, estimated PGA_{EMS} amplification factors relative to AB03 reveal systematic deamplification in the central valley, where sediment thickness is deepest (e.g. Paudyal et al. 2012). Deamplification factors in the central valley relative to adjacent foothills are generally in the range 0.6–0.9. The former result is consistent with the conclusions that sediments in the Kathmandu Valley experienced a pervasively non-linear response during the mainshock (Dixit et al. 2015; Rajaure et al. 2016).

At regional distances, significant PGA_{EMS} amplification is observed throughout the southern Indo-Gangetic basin, consistent with expectations and past studies (e.g. Hough and Bilham 2008). To the south of the mainshock rupture, deamplified shaking suggests a significant source effect that is consistent with an expected directivity effect. The occurrence of the $M_{\text{W}}7.3$ Dolakha aftershock on 12 May 2015 along the eastern edge of the rupture is also consistent with enhanced shaking in the along-strike direction. Gomberg et al. (2003) showed that aftershocks preferentially cluster in the forward directivity direction.

We conclude that the overall distribution of ground motions from the Gorkha earthquake was controlled by a complex combination of source, path, and site effects. The extensive intensity data set determined by Martin et al. (2015) provides a unique, spatially rich characterization of ground motions that will be a critical base of comparison for future modelling studies.

2.1 Data and resources

Intensity data for the Gorkha earthquakes are available as an electronic supplement to Martin et al. (2015). Strong motion data from KATNP and DMG stations are freely available from <http://www.strongmotioncenter.org> (last accessed January 28, 2016), and as an electronic supplement to Bhattarai et al. (2015). Figure 8 was produced using the freely available QGIS 2.10 software, and all other figures were prepared using the freely available GMT software.

Acknowledgments We are thankful for helpful conversations with Pablo Ampuero, Domniki Asimaki, Aron Meltzner, and Sudhir Rajaura, to Eric Thompson for providing predicted PGA values for the BSSA14 GMPE, to Gail Atkinson for providing predicted PGA values for the Ghofrani and Atkinson (2014) GMPE, and to Christina Widiwijayanti for providing us a copy of Ohsumi et al. (2016). We are further grateful to Aron Meltzner and Bruce Worden for constructive reviews of an earlier version of this manuscript, and to two anonymous reviewers for their constructive reviews. SEH was supported by the Office of US Foreign Disaster Assistance (OFDA), a branch of the US Agency for International Development (USAID). SSM was supported by Kerry Sieh through the National Research Foundation Singapore and the Singapore Ministry of Education under the Research Centres of Excellence initiative. This work comprises Earth Observatory of Singapore contribution no. 116.

References

- Ambraseys NN, Bilham R (2003a) Reevaluated intensities for the great Assam earthquake of 12 June 1897, Shillong, India. *Bull Seism Soc Am* 93(2):655–673. doi:[10.1785/0120020093](https://doi.org/10.1785/0120020093)
- Ambraseys NN, Bilham R (2003b) Earthquakes and associated deformation in northern Baluchistan 1892–2001. *Bull Seism Soc Am* 93(2):1573–1605. doi:[10.1785/0120020038](https://doi.org/10.1785/0120020038)
- Ambraseys N, Douglas JJ (2004) Magnitude calibration of north Indian earthquakes. *Geophys J Int* 159(1):165–206. doi:[10.1111/j.1365-246X.2004.02323.x](https://doi.org/10.1111/j.1365-246X.2004.02323.x)
- Ampuero J-P, Hough SE, Meng L, Thompson EM, Zhang A, Martin SS, Asimaki D, Inbal A (2016) Damage limited by the distribution of high-frequency radiation in the 2015 Gorkha, Nepal, Earthquake (in review)
- Atkinson GM, Boore DM (2003) Empirical ground-motion relations for subduction zone earthquakes and their application to Cascadia and other regions. *Bull Seism Soc Am* 93:1703–1729. doi:[10.1785/0120020156](https://doi.org/10.1785/0120020156)
- Avouac J-P, Meng L, Wei S, Wang T, Ampuero J-P (2015) Unzipping lower edge of locked Main Himalayan thrust during the 2015, Mw7.8 Gorkha earthquake. *Nat Geosci* 8:708–711. doi:[10.1038/ngeo2518](https://doi.org/10.1038/ngeo2518)
- Bakun WH, Wentworth CM (1997) Estimating earthquake location and magnitude from seismic intensity data. *Bull Seism Soc Am* 87:1502–1521
- Bhattarai M, Adhikari LB, Gautam UP, Laurendeau A, Labonne C, Hoste-Colomer R, Sebe O, Hernandez B (2015) Overview of the large 25 April 2015 Gorkha, Nepal, earthquake from accelerometric perspectives. *Seismol Res Lett* 86:1540–1548. doi:[10.1785/0220150140](https://doi.org/10.1785/0220150140)
- Bilham R (1999) Location and magnitude of the 1833 Nepal earthquake and its relation to the rupture zones of contiguous great Himalayan earthquakes. *Curr Sci* 69(2):155–187
- Bollinger L, Sapkota SN, Tapponnier P, Klinger Y, Rizza M, Van Der Woerd J, Tiwari DR, Pandey R, Bitri A, Bes de Berc S (2014) Estimating the return times of great Himalayan earthquakes in eastern Nepal: evidence from the Patu and Bardibas strands of the main frontal thrust. *J Geophys Res* 119:7123–7163. doi:[10.1002/2014JB010970](https://doi.org/10.1002/2014JB010970)
- Bollinger L, Tapponnier P, Sapkota SN, Klinger Y (2016) Slip deficit in central Nepal: omen for a repeat of the 1344 AD earthquake? *Earth Planet Sp* 68:12. doi:[10.1186/s40623-016-0389-1](https://doi.org/10.1186/s40623-016-0389-1)
- Boore DM (1983) Stochastic simulation of high-frequency ground motions based on seismological models of radiated spectra. *Bull Seism Soc Am*. 73:1865–1894
- Boore DM, Stewart JP, Seyhan E, Atkinson GM (2014) Nga-west2 equations for predicting pga, pgv, and 5% damped psa for shallow crustal earthquakes. *Earthq Spectr* 30(3):1057–1085
- Bossu R, Landès R, Roussel F, Steed R, Mazet-Roux R, Martin SS, Hough SE (2016) Thumbnail-based questionnaires for the rapid and efficient collection of macroseismic data from global earthquakes. *Seism Res Lett* (in review)
- Caprio M, Tarigan B, Worden CB, Wiemer S, Wald DJ (2015) Ground motion to intensity conversion equations (GMICEs): a global relationship and evaluation of regional dependency. *Bull Seism Soc Am*. 106:2. doi:[10.1785/0120140286](https://doi.org/10.1785/0120140286)
- Chadha RK, Srinagesh D, Srinivas D, Suresh G, Sateesh A, Singh SK, Pérez-Campos X, Suresh G, Koketsu K, Masuda T, Domen K, Ito T (2015) CIGN, a strong motion seismic network in central Indo-Gangetic plains, foothills of Himalayas: first results. *Seismol Res Lett* 87:37–46. doi:[10.1785/0220150106](https://doi.org/10.1785/0220150106)
- Chaulagain H, Rodrigues H, Silva V, Spacone E, Varum H (2015) Seismic risk assessment and hazard mapping in Nepal. *Nat Hazards* 78(1):583–602
- Chen, J. et al. (1982). 西藏地震史料汇编: 公元642年 - 1980年 (A collection of material on earthquakes in Tibet: 642–1980), 西藏自治区科学技术委员会, 西藏人民出版社, 1, 39–76, Lhasa

- Dixit AM, Ringler A, Sumy D, Cochran E, Hough SE, Martin SS, Gibbons S, Luetgert J, Galetzka J, Shrestha SN, Rajaure S, McNamara D (2015) Strong motion recordings of the M7.8 Gorkha, Nepal, earthquake sequence from low-cost, Quake Catcher Network accelerometers. *Seismol Res Lett* 86(6):1533–1539. doi:[10.1785/0220150146](https://doi.org/10.1785/0220150146)
- Galetzka J, Melgar D, Genrich JF, Geng J, Owen S, Lindsey EO, Xu X, Bock Y, Avouac J-P, Adhikari L-B, Upreti BN, Pratt-Sitaula B, Bhattarai TN, Sitaula B, Moore A, Hudnut KW, Szeliga W, Normandeau J, Fend M, Flouzat M, Bollinger L, Shrestha P, Koirala B, Gautam U, Bhattarai M, Gupta R, Kandel T, Timsina C, Sapkota SN, Rajaure S, Maharjan N (2015) Slip pulse and resonance of Kathmandu basin during the 2015 Mw7.8 Gorkha earthquake, Nepal, imaged with space geodesy. *Science* 349:1091–1095. doi:[10.1126/science.aac6383](https://doi.org/10.1126/science.aac6383)
- Ghofrani H, Atkinson GM (2014) Ground-motion prediction equations for interface earthquakes of M7 to 9 in Japan based on empirical data. *Bull Earthq Eng* 12:549–571. doi:[10.1007/s10518-013-9533-5](https://doi.org/10.1007/s10518-013-9533-5)
- Gomberg J, Bodin P, Reasenber P (2003) Observing earthquakes triggered in the near field by dynamic deformations. *Bull Seism Soc Am* 93:118–138. doi:[10.1785/0120020075](https://doi.org/10.1785/0120020075)
- Grünthal G (ed) (1998) *The European Macroseismic Scale EMS-98*, vol 15. Conseil de l'Europe, Cahiers du Centre Européen de Géodynamique et de Seismologie, Luxembourg, p 101
- Hanks TC, Johnston AC (1992) Common features of the excitation and propagation of strong ground motion for North American earthquakes. *Bull Seism Soc Am* 82:1–23
- Hashash YMA, Tiwari B, Moss RES, Asimaki D, Clahan KB, Kieffer DS, Dreger DS, McDonald A, Madugo CM, Mason HB, Pehlivan M, Rayamajhi D, Acharya I, Adhikari B (2015) Geotechnical field reconnaissance: Gorkha (Nepal) earthquake of April 25, 2015 and related shaking sequence. Geotechnical extreme event reconnaissance GEER Association Report No. GEER-040, 1
- Hauksson E, Felzer K, Given D, Giveon M, Hough SE, Hutton K, Kanamori H, Sevilgen V, Wei S, Yong A (2008) Preliminary report on the 29 July 2008 Mw 5.4 Chino Hills, eastern Los Angeles basin, California, earthquake sequence. *Seismol Res Lett* 79:855–866. doi:[10.1785/gssrl.79.6.85](https://doi.org/10.1785/gssrl.79.6.85)
- Hossler T, Bollinger L, Sapkota SN, Lavé J, Gupta RM, Kandel TP (2016) Surface ruptures of large Himalayan earthquakes in western Nepal: evidence along are activated strand of the main boundary thrust. *Earth Planet Sci Lett* 187–196. doi:[10.1016/j.epsl.2015.11.042](https://doi.org/10.1016/j.epsl.2015.11.042)
- Hough SE (2012) Initial assessment of the intensity distribution of the 2011 Mw5.8 Mineral, Virginia, earthquake. *Seismol Res Lett* 83(4):649–657. doi:[10.1785/0220110140](https://doi.org/10.1785/0220110140)
- Hough SE (2014) Shaking from injection-induced earthquakes in the central and eastern United States. *Bull Seism Soc Am* 104:2767–2781. doi:[10.1785/0120120285](https://doi.org/10.1785/0120120285)
- Hough SE (2015) Introduction to the focus section on the 2015 Gorkha, Nepal, Earthquake. *Seismol Res Lett* 86:1502–1505. doi:[10.1785/0220150212](https://doi.org/10.1785/0220150212)
- Hough SE, Bilham R (2008) Site response of the Ganges basin inferred from re-evaluated macroseismic observations from the 1897 Shillong, 1905 Kangra, and 1934 Nepal earthquakes. *J Earth Syst Sci* 117:773–782. doi:[10.1007/s12040-008-0068-0](https://doi.org/10.1007/s12040-008-0068-0)
- Hough SE, Pande P (2007) The 1868 Hayward fault, California, earthquake: implications for earthquake scaling relations on partially creeping faults. *Bull Seism Soc Am* 97:638–645. doi:[10.1785/0120060072](https://doi.org/10.1785/0120060072)
- Iyengar RN (1999) Earthquakes in ancient India. *Curr Sci* 77(6):827–829
- Karakaş C, Tapponnier P, Sapkota SN, Klinger Y, Coudurier-Curveur A, Ildefonso S, Gao M, Bollinger L (2015) High resolution topography and multiple seismic uplift on the main frontal thrust near the ratu river, eastern Nepal, In: Asia-Oceania geophysical society annual meeting, Abstract SE17-D5-PM2-P-006
- Kumar A, Mittal H, Sachdeva R, Kumar A (2015) Indian strong motion instrumentation network. *Seism Res Lett* 83:59–66. doi:[10.1785/gssrl.83.1.59](https://doi.org/10.1785/gssrl.83.1.59)
- Lavé J, Yule D, Sapkota S, Basant K, Madden C, Attal M, Pandey R (2005) Evidence for a great Medieval earthquake (1100 A.D.) in the central Himalayas, Nepal. *Science* 307(5713):1302–1305. doi:[10.1126/science.1104804](https://doi.org/10.1126/science.1104804)
- Lindsey EO, Natsuaki R, Xu X, Shimada M, Hashimoto M, Melgar D, Sandwell DT (2015) Line-of-sight displacement from ALOS-2 interferometry: Mw7.8 Gorkha earthquake and Mw7.3 aftershock. *Geophys Res Lett* 42(16):6655–6661. doi:[10.1002/2015GL065385](https://doi.org/10.1002/2015GL065385)
- Martin S, Hough SE (2015) The 2014 Bay of Bengal earthquake: macroseismic data reveals a high-stress drop event. *Seism Res Lett* 86(2A):369–377. doi:[10.1785/0220140155](https://doi.org/10.1785/0220140155)
- Martin SS, Hough SE (2016) Reply to, “Comment on ‘Ground Motions from the 2015 Mw 7.8 Gorkha, Nepal, Earthquake Constrained by a Detailed Assessment of Macroseismic Data’ by Stacey Martin, Susan E. Hough and Charleen Hung” by Andrea Tertulliani, Laura Graziani, Corrado Castellano, Alessandra Maramai, Antonio Rossi. *Seism Res Lett* 87:957–962. doi:[10.1785/0220160061](https://doi.org/10.1785/0220160061)

- Martin S, Kakar DM (2012) The 19 January 2011 Mw 7.2 Dalbandin earthquake, Balochistan. *Bull Seism Soc Am* 100(4):1810–1819. doi:[10.1785/0120110221](https://doi.org/10.1785/0120110221)
- Martin S, Szeliga W (2010) A catalog of felt intensity data for 589 earthquakes in India, 1636–2009. *Bull Seism Soc Am* 100(2):536–569. doi:[10.1785/0120080328](https://doi.org/10.1785/0120080328)
- Martin S, Hough SE, Hung C (2015) Ground motions from the 2015 M_w 7.8 Gorkha, Nepal, earthquake constrained by a detailed assessment of macroseismic data. *Seism Res Lett* 86:1524–1532. doi:[10.1785/0220150138](https://doi.org/10.1785/0220150138)
- Medvedev SV, Sponheuer W, Kárník V (1965) Шкала Сейсмической Интенсивности MSK 1964 (*Seismic Intensity Scale Version MSK 1964, in Russian*). Ком., Moscow, AkademiiNauk SSSR Geofiz, p 280
- Meltzner AJ, Wald DJ (1998) Foreshocks and aftershocks of the great 1857 California earthquakes, U.S. Geological Survey Open File Report, 1998—465, pp 111–112
- Meltzner AJ, Wald DJ (2002) Felt reports and intensity assignments for aftershocks and triggered events of the great 1906 California earthquake, U.S. Geological Survey Open File Report, 2002–37, p 299
- Meng L, Zhang A, Yagi Y (2016) Improving back-projecting imaging with a novel physics-based aftershock calibration approach: a case study of the 2015 Gorkha earthquake. *Geophys Res Lett* 43(2):628–636. doi:[10.1002/2015GL067034](https://doi.org/10.1002/2015GL067034)
- Mitra S, Paul H, Kumar A, Singh SK, Dey S, Powali D (2015) The 25 April 2015 Nepal earthquake and its aftershocks. *Curr Sci* 108(10):1938–1943
- Mugnier JL, Gajurel AP, Huyghe P, Becel D (2005) Frontal and piggy-back seismic ruptures in the external thrust belt of Western Nepal. *J Asian Earth Sci* 25(5):707–717. doi:[10.1016/j.jseaes.2004.05.009](https://doi.org/10.1016/j.jseaes.2004.05.009)
- Murphy MA, Taylor MH, Goss J, Silver CRP, Whipp DM, Beaumont C (2014) Limit of strain partitioning in the Himalaya marked by large earthquakes in western Nepal. *Nat Geosci* 7:38–42. doi:[10.1038/ngeo2017](https://doi.org/10.1038/ngeo2017)
- Musson R (1998) Intensity assignments from historical earthquake data: issues of certainty and quality. *Annali di Geofisica* 41(1):79–91
- Musson RMW, Grunthal G, Stucchi M (2010) The comparison of macroseismic intensity scales. *J Seismol* 14:413–428. doi:[10.1007/s10950-009-9172-0](https://doi.org/10.1007/s10950-009-9172-0)
- Ohsumi T, Hiroshi I, Inoue H, Aoi S, Fujiwara H (2016) Investigation of damage in and around Kathmandu Valley related to the 2015 Gorkha, Nepal earthquake. In: Technical note of the national research institute for earth science and disaster prevention, 404
- Oldham T (1883) A catalogue of Indian earthquakes from the earliest time to the end of A.D. 1869. *Memoir Geol Sur India* 29:163–215
- Pande P, Kayal JR (eds.) (2003) Kutch (Bhuj) earthquake 26 January 2001. Geological survey of India, Special Publication 76, Lucknow
- Paudyal YR, Yatabe R, Bhandary N, Dahal R (2012) A study of local amplification effect of soil layers on ground motion in the Kathmandu valley using microtremor analysis. *Earthq Eng Eng Vib* 11(2):257–268
- Prakash R, Singh RK, Srivastava HN (2016) Nepal earthquake 25 April 2015: source parameters, precursory pattern and hazard assessment. *Geomat Nat Hazard Risk*. doi:[10.1080/19475705.2016.1155504](https://doi.org/10.1080/19475705.2016.1155504)
- Rajaure S, Asimaki D, Thompson EM, Hough S, Martin S, Ampuero JP, Inbal A, Dhital MR, Paudel L (2016) Strong motion observations of the Kathmandu valley response during the M7.8 Gorkha earthquake sequence, in review. *Tectonophysics*
- Sapkota SN, Bollinger L, Klinger Y, Tapponnier P, Gaudemer Y, Tiwari D (2013) Primary surface rupture of the great Himalayan earthquakes of 1255 and 1934. *Nat Geosci* 6:71–76. doi:[10.1038/ngeo1669](https://doi.org/10.1038/ngeo1669)
- Singh SK, Mena E, Castro R (1988) Some aspects of source characteristics of the 19 September 1985 Michoacan earthquake and ground motion amplification in and near Mexico City from strong motion data. *Bull Seism Soc Am* 78(2):451–477
- Smith-Baird R (1844) Memoir on Indian earthquakes. *J Asiat Soc Bengal* 12:257–293
- Szeliga W, Hough SE, Martin S, Bilham R (2010) Intensity, magnitude, location, and attenuation in India for felt earthquakes since 1762. *Bull Seism Soc Am* 100:570–584. doi:[10.1785/0120080329](https://doi.org/10.1785/0120080329)
- Takai N, Shigefuji M, Rajaure S, Bijukchhen S, Ichiyonagi M, Dhital MR, Sasatani T (2016) Strong ground motion in the Kathmandu valley during the 2015 Gorkha, Nepal, earthquake. *Earth Planet Sp* 68:1. doi:[10.1186/s40623-016-0383-7](https://doi.org/10.1186/s40623-016-0383-7)
- Tertulliani A, Graziani L, Castellano C, Maramai A, Rossi A (2016) Comment on ‘Ground Motions from the 2015 Mw 7.8 Gorkha, Nepal, Earthquake Constrained by a Detailed Assessment of Macroseismic Data’ by Stacey Martin, Susan E. Hough and Charleen Hung. *Seism Res Lett*. doi:[10.1785/0220150258](https://doi.org/10.1785/0220150258)
- Topozada TR, Real CR (1981) Preparation of isoseismal maps and summaries of Reported Effects for pre-1900 California earthquakes. U.S. Geological Survey Open File Report, 1981–262, p 7–11

- Udhoji et al. (2000). Jabalpur earthquake 22 May 1997—a geoscientific study, Special Publication 51, Geological Survey of India, Government of India, 2000
- Wald DJ, Quitoriano V, Dengler L, Dewey JW (1999) Utilization of the internet for rapid community intensity maps. *Seism Res Lett* 70(6):680–697. doi:[10.1785/gssrl.70.6.680](https://doi.org/10.1785/gssrl.70.6.680)
- Worden CB, Wald DJ, Lin K, Cua G, Garcia D (2010) A revised ground-motion and intensity interpolation scheme for shakemap. *Bull Seism Soc Am* 100:3083–3096. doi:[10.1785/0120100101](https://doi.org/10.1785/0120100101)
- Worden CB, Gerstenberger MC, Rhoades DA, Wald DJ (2012) Probabilistic relationships between ground-motion parameters and modified Mercalli intensity in California. *Bull Seism Soc Am* 102:204–221. doi:[10.1785/0120110156](https://doi.org/10.1785/0120110156)
- Zuccaro G, Cacace F, de Gregorio D (2012) Buildings inventory for seismic vulnerability assessment on the basis of Census data assessment at national and regional scale, 15WCEE, Lisbon